



**A Finite Element Benchmark for the Dynamic
Analysis of Perforated Plates with a Square
Penetration Pattern**

D.L. Kaap, M.A. Sprague, R.L. Engelstad

May 1997

UWFDM-1034

FUSION TECHNOLOGY INSTITUTE

UNIVERSITY OF WISCONSIN

MADISON WISCONSIN

**A Finite Element Benchmark for the Dynamic
Analysis of Perforated Plates with a Square
Penetration Pattern**

D.L. Kaap, M.A. Sprague, R.L. Engelstad

Fusion Technology Institute
University of Wisconsin
1500 Engineering Drive
Madison, WI 53706

<http://fti.neep.wisc.edu>

May 1997

UWFDM-1034

Table of Contents

1. Introduction	1
<i>1.1 Background</i>	1
<i>1.2 Motivation</i>	2
2. Plate Terminology and Perforation Geometry	3
<i>2.1 Nomenclature</i>	3
<i>2.2 Geometry of the Perforation Pattern</i>	4
3. Finite Element Model Development and Verification	5
<i>3.1 Classical Plate Theory - Static Loading</i>	5
<i>3.2 Classical Plate Theory - Dynamic Loading</i>	5
<i>3.3 Thin Plate Theory</i>	6
<i>3.4 Geometric Modeling and Meshing</i>	6
<i>3.5 Nodal Loading</i>	7
<i>3.6 Finite Element Results - Solid Plate</i>	8
<i>3.7 Finite Element Results - Perforated Plate</i>	10
4. Dynamic Analysis of Perforated Plates	11
<i>4.1 Dynamic Effective Material Constants</i>	11
<i>4.2 Finite Element Results</i>	11
5. Conclusions	12
6. References	15

1. Introduction

1.1 Background

Perforated plates and shells are used in a variety of industrial applications. Some examples include nozzles, material or fluid screens, and heat exchangers. Most of these applications incorporate a design based on classical plate or shell theory and employ static loading only. Of these, the heat exchanger (Fig. 1) is the most documented. The tubes in a heat exchanger are held in place by a perforated plate called a tube sheet (Fig. 2). The structural deficiencies caused by the perforations in this sheet are accounted for by using “effective” material properties. The idea of using “effective” material properties, based on theoretical and experimental work, first started in 1948 and has since evolved into an industry standard for the design of tubesheets [1].

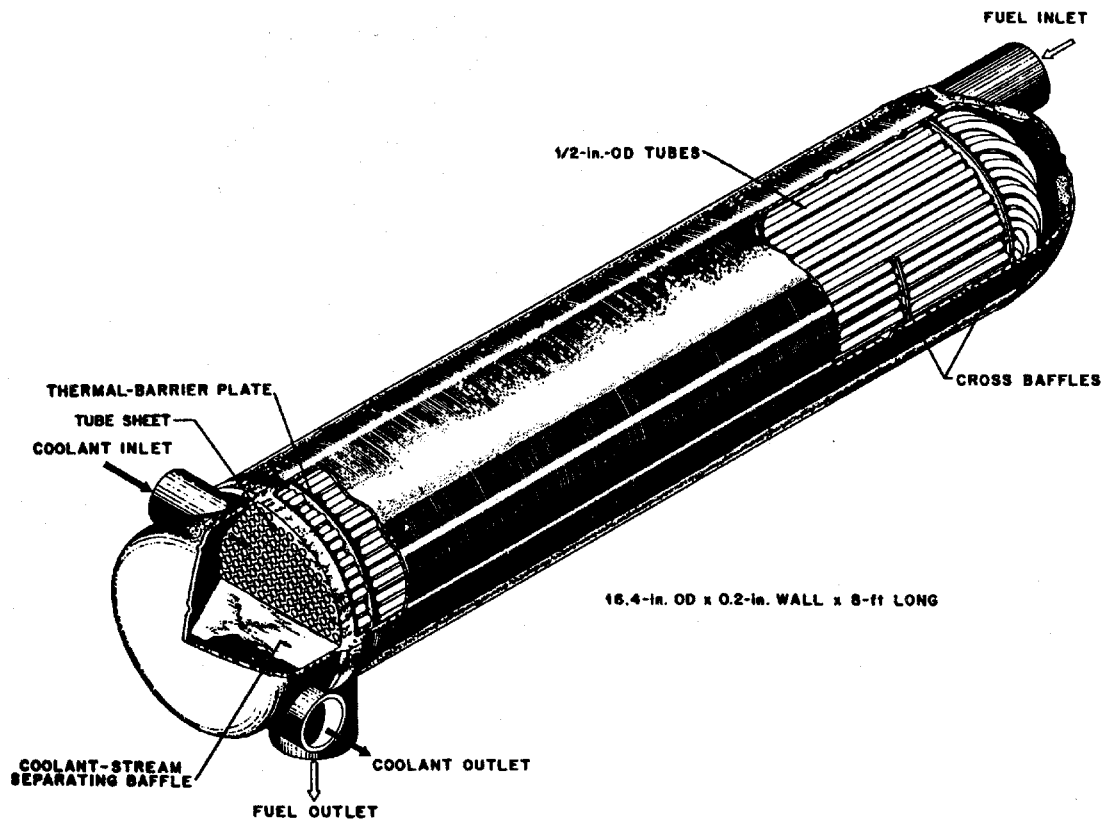


Fig. 1. Heat exchanger with cutaway showing tube sheet [2].

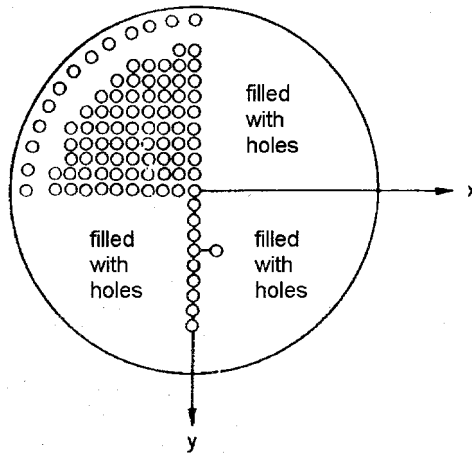


Fig. 2. Tube sheet from heat exchanger [3].

1.2 Motivation

Every paper published in the past 80 years documenting the structural design or analysis of perforated structures has focused on either experimental data generated from statically loaded plates or on theories related to the static analysis of perforated plates. Even papers dealing with the dynamic analysis of shells have used effective material properties generated from static loading. One example of this is the Light Ion Microfusion Facility (LMF) cylindrical shell (Figs. 3 and 4) analyzed by Powers [4]. The current research addresses the accuracy in using “static-plate” effective material properties in a dynamic analysis.

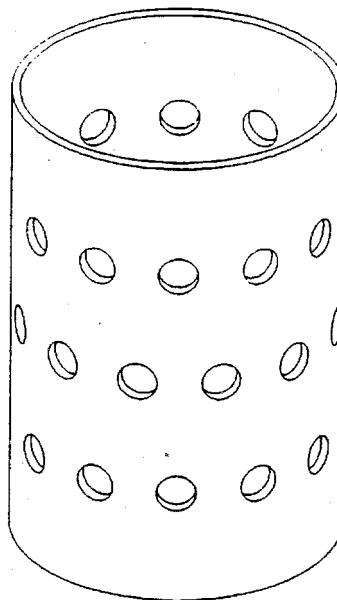


Fig. 3. Perforated cylindrical target chamber from LMF [4].

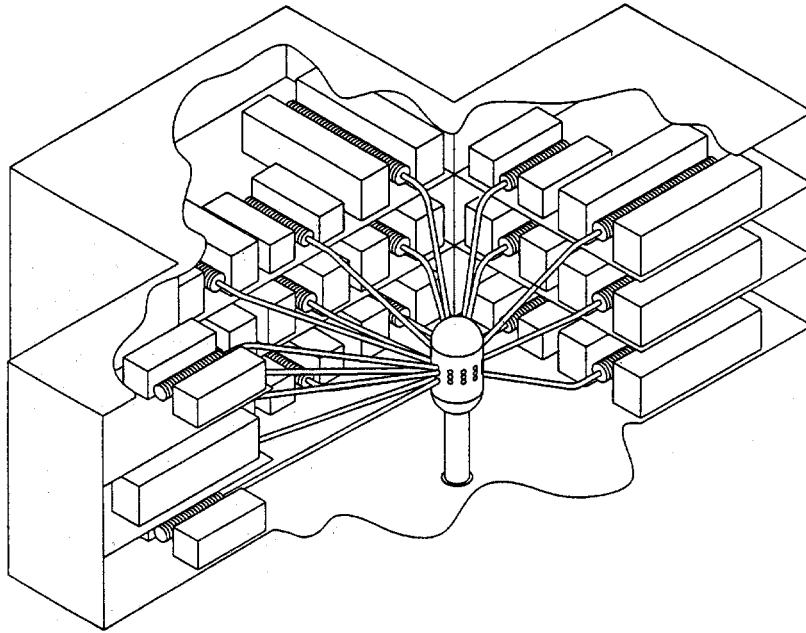


Fig. 4. Light Ion Microfusion Facility (LMF) [5].

2. Plate Terminology and Perforation Geometry

2.1 Nomenclature

a	plate width, in
b	plate length, in
t	plate thickness, in
h	hole-edge to hole-edge distance, in
R	radius of perforations, in
P	pitch, in.
μ	ligament efficiency $[1 - \frac{d}{P}]$
D	bending stiffness $[\frac{E^* h^3}{12 * (1 - \nu^2)}]$, lb-in
D^*	effective bending stiffness, lb-in
	mass per unit area, $\text{lb-s}^2/\text{in}^4$
E	Young's modulus, psi
E^*	effective Young's modulus, psi
ν	Poisson's ratio
ν^*	effective Poisson's ratio
M_o	edge moment per unit length on plate, lb-in/in
x, y, z	rectangular coordinates
r, θ, z	polar coordinates

w	deflection of plate perpendicular to the x - y plane, in
w_{FEM}	deflection of plate derived using finite element methods, in
w_{theory}	deflection of plate derived using statically developed material properties, in
f_{FEM}	frequency derived using finite element methods, Hz
f_{theory}	frequency derived using statically developed effective material properties, Hz
ω_{FEM}	circular frequency derived using finite element methods, rad/s
ω_{theory}	circular frequency derived using statically developed effective material properties, rad/s
n, m	modal half waves corresponding to directions x and y , respectively
$\{r_e\}$	load vector for consistent nodal loading, lb-in
q	loading per unit length, lb-in/in
$[N]^T$	element shape function

2.2 Geometry of the Perforation Pattern

Two geometry patterns, square and triangular, are used in industrial applications, but only the square pattern (Fig. 5) is considered here. This pattern, as well as the triangular pattern, is determined fully by one parameter, μ , referred to as the ligament efficiency (see the nomenclature list in Section 2.1).

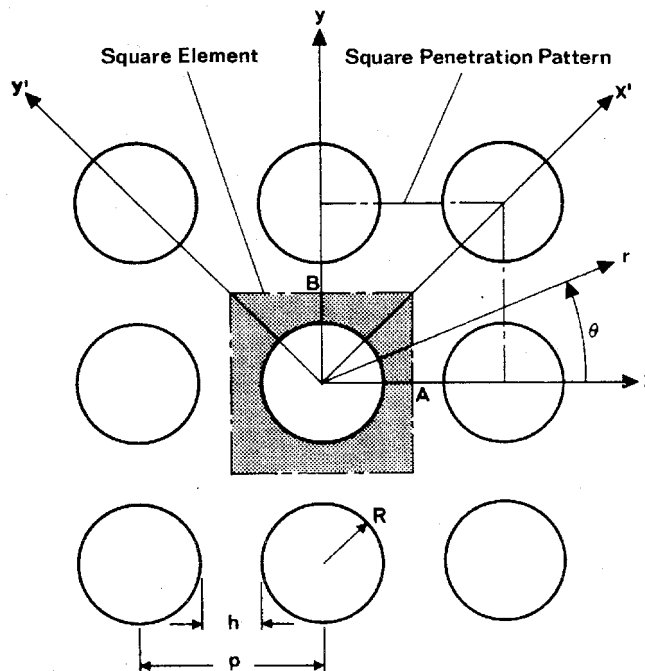


Fig. 5. Square perforation pattern geometry [6].

3. Finite Element Model Development and Verification

3.1 Classical Plate Theory - Static Loading

Simply supported perforated plates have been used in the past to generate “static-plate” effective material properties and thus, are used here as a benchmark for the finite element (FE) models. More specifically, the following analysis utilizes a simply supported rectangular plate subjected to symmetrically distributed edge moments at $y = \pm \frac{b}{2}$ (Fig.

6). The uniformly distributed edge moments per unit length, M_o , are statically applied, resulting in a transverse deflection w . This deflection can be determined experimentally [8], or, in the case of this paper, numerically with the FE software ANSYS. By substituting this deflection data, along with plate dimensions and applied edge moments, into a relationship for the deflection of a square plate, the corresponding stiffness, D , may be found. Ugural [9] represents the solution for the deflection of a simply supported square plate with an infinite series, i.e.,

$$w(x, y) = \frac{2M_o a}{\pi^2 D} \sum_{m=1,3,\dots}^{\infty} \frac{\sin(m\pi x/a)}{m^2 \cosh \alpha_m} \left(\frac{b}{2} \tanh \alpha_m \cosh \frac{m\pi y}{a} - y \sinh \frac{m\pi y}{a} \right)$$

where $\alpha_m = \frac{m\pi b}{2a}$. When perforated plates are subsequently evaluated, the effective stiffness, D^* , can then be determined by the same procedure.

3.2 Classical Plate Theory - Dynamic Loading

The natural frequencies of the benchmarked plate models were obtained by running a modal analysis on each model using ANSYS. As with the static case the stiffness, D , of the plate can be found by substituting known values, such as natural frequency and mode number, into a relationship for the frequency of a square plate. The vibration of thin, simply supported plates (Fig. 6) is described by the following shape function and frequency equation [10], respectively,

$$W(x, y) = X(x)Y(y) = \sum_{m=1}^{\infty} \sum_{n=1}^{\infty} W_{m,n} \sin \frac{m\pi x}{a} \sin \frac{n\pi y}{b} \quad (m = 1,2,3,\dots \text{ and } n = 1,2,3,\dots)$$

$$\omega_{m,n} = \pi^2 \left[\frac{m^2}{a^2} + \frac{n^2}{b^2} \right] \sqrt{\frac{D}{m}} \quad (m = 1,2,3,\dots \text{ and } n = 1,2,3,\dots)$$

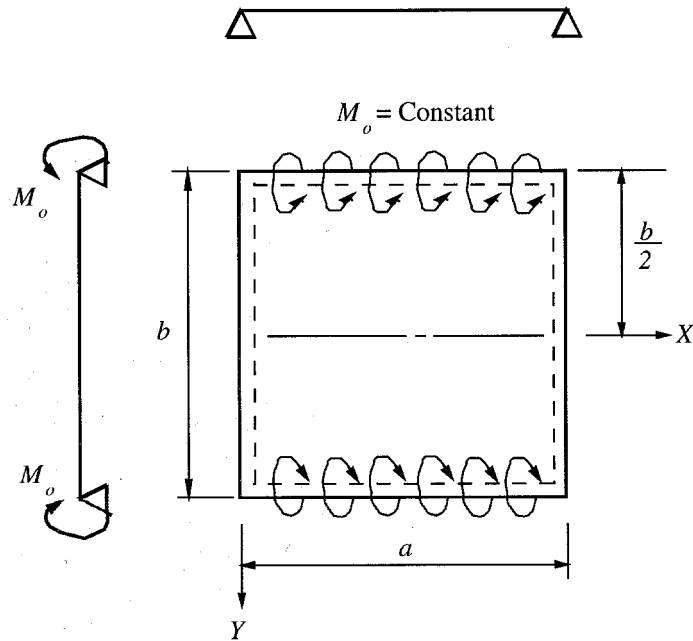


Fig. 6. View of simply-supported plate with edge moments.

3.3 Thin Plate Theory

The work done in this paper focuses on plates but the intent is to transfer the knowledge gained to the dynamic analysis of a shell, such as the LMF chamber. Such a transfer of information requires as much similarity as possible between the shell and the plate. For example, thin plates are used because the above mentioned shells are thin-walled, e.g.,

$$\frac{t}{R} \leq \frac{1}{20}. \text{ Thin plate theory requires that } \frac{h}{b} \leq \frac{1}{20}.$$

3.4 Geometric Modeling and Meshing

The FE model should accurately represent the number of holes, the perforation geometry of the holes, the plate thickness, and the boundary conditions. In addition, a large number of holes should be used to approximate an infinite plate. An infinite plate is desirable in perforated plate analysis because the irregularities around the supported edges are “washed out.”

Models constructed within ANSYS were also meshed within ANSYS. Of the 120 different elements available only a few were considered. By using thin plates, as discussed previously, the number of possible elements applicable to this analysis was reduced to two shell elements (see Table 1). The optimal mesh pattern, using either element, is shown in Fig. 7 [11]. Figure 7 does not necessarily display a optimum mesh density.

Table 1. Comparison of ANSYS shell elements.

Element Name	No. of Nodes	No. of Nodal D.O.F	Deformation Shape	Important Characteristics
SHELL63	4	6	Linear in both in-plane directions	Includes bending and membrane capabilities.
SHELL93	8	6	Quadratic in both in-plane directions	Mid-side node makes this element well suited to model curvature around holes. It includes bending and membrane capabilities. Non-linear capabilities include stress stiffening and large deflection theory.

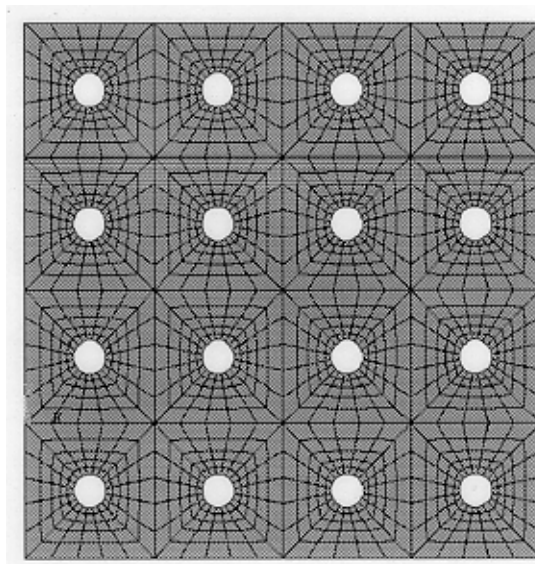


Fig. 7. Full square-pattern plate model meshed on ANSYS.

3.5 Nodal Loading

Moment distributions on parallel edges must be applied at nodes in such a way as to simulate a uniform edge moment. Consistent nodal loading does this. When used correctly the deflection contours for the simply supported plate will look like the ones in Fig. 8. Consistent nodal loading for 4-node and 8-node elements is shown in Fig. 9. They are calculated using the following [12]:

$$\{r_e\} = \int_0^L [N]^T q ds$$

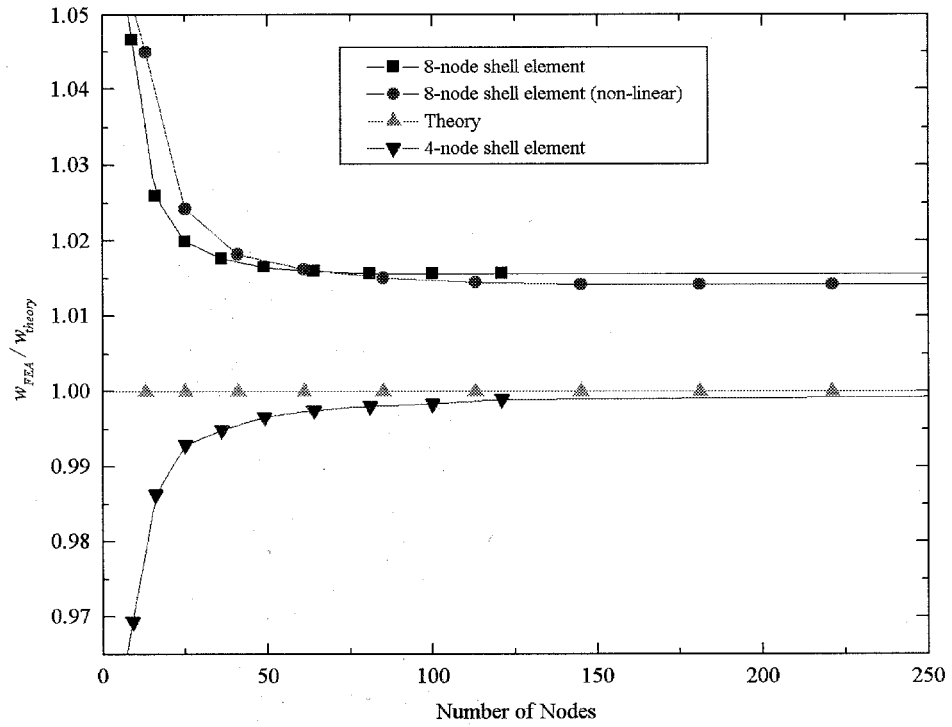


Fig. 10. Mesh convergence for static loading of solid plate.

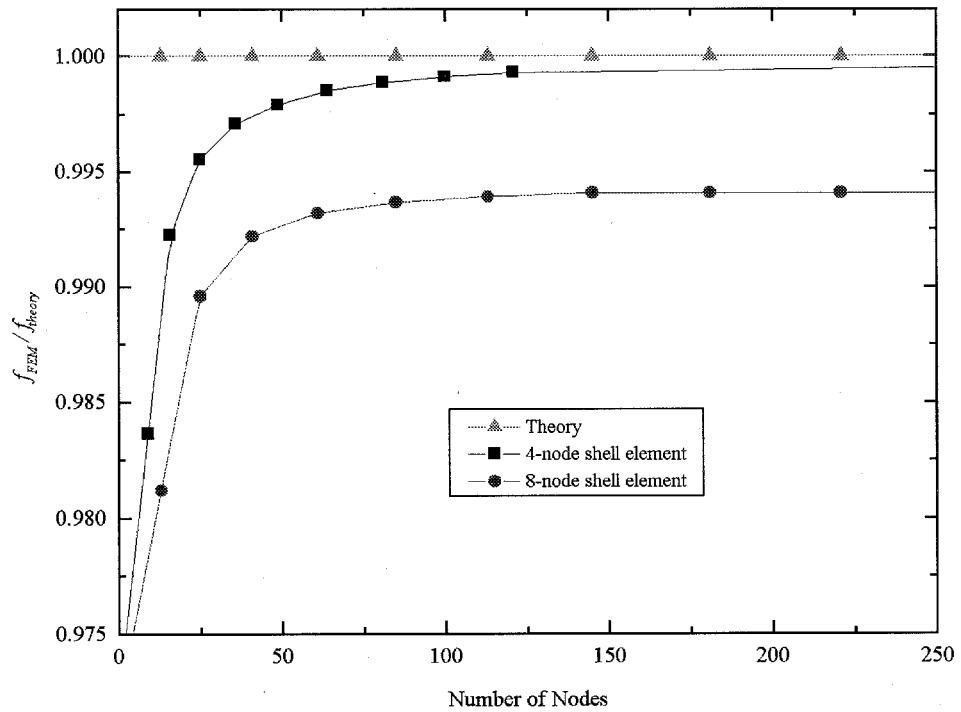


Fig. 11. Mesh convergence for dynamic loading (mode 1,1) of solid plate.

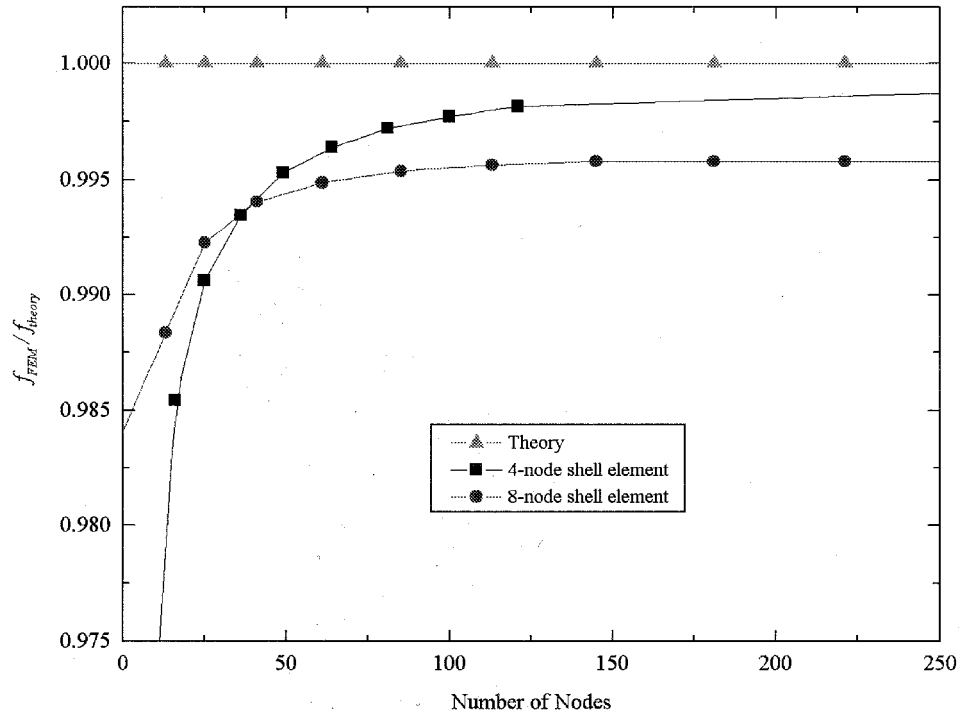


Fig. 12. Mesh convergence for dynamic loading (mode 1,3) of solid plate.

Table 2. Comparison of error convergence for solid plate.

Analysis Type	Element	Total Nodes	Percentage Error
Static	4-node	841	0.0215%
Static	8-node	841	1.5595%
Static	8-node nonlinear	841	1.3870%
Dynamic	4-node (mode 1,1)	841	0.0100%
Dynamic	8-node (mode 1,1)	841	0.5921%
Dynamic	4-node (mode 1,3)	841	0.0437%
Dynamic	8-node (mode 1,3)	841	0.4206%

3.7 Finite Element Results - Perforated Plate

The FE results for the static deflection of two different perforated plates were compared to calculated deflections based on published data for static effective constants. The two plates were identical except for perforation hole size (also quantified as ligament efficiency). Using a 4-node shell element and mesh refinement, FE results with smaller ligament efficiencies converge to the published data. However, FE results become smaller than published data as ligament efficiency increases, showing a 4.3 % deviation at a ligament efficiency of 1.60 (Fig. 13).

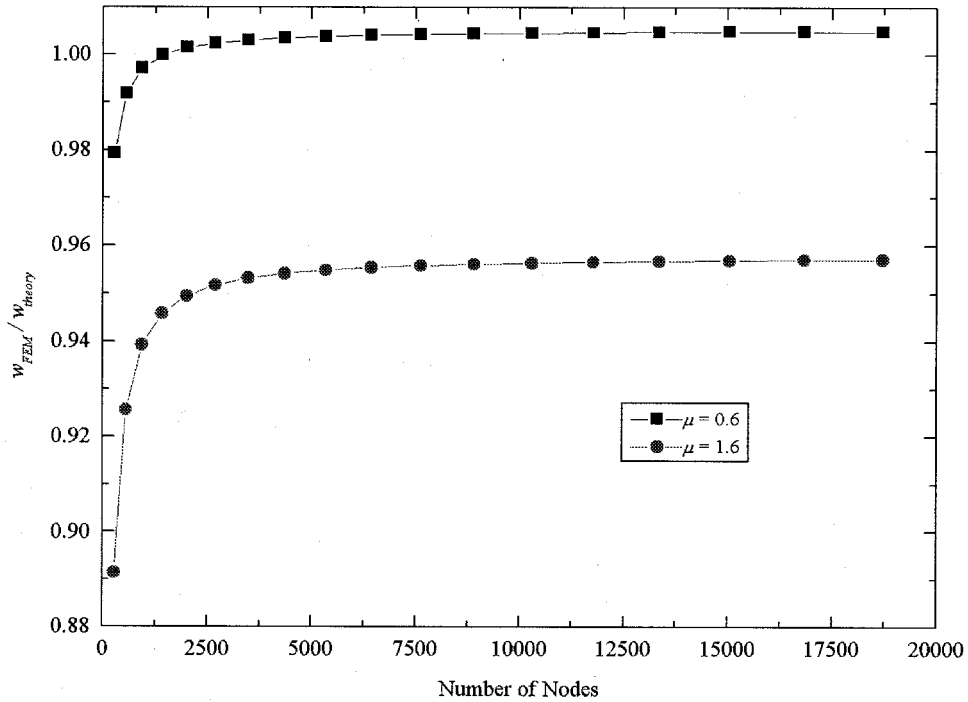


Fig. 13. Mesh convergence for static loading of perforated plate using 4-node element (ANSYS SHELL63).

4. Dynamic Analysis of Perforated Plates

4.1 Dynamic Effective Material Constants

Effective material constants developed over the past 50 years have been based on static criteria. Experimentally, these constants have been calculated using deflection data [13]. These deflections are then substituted into a governing equation for deflection (found in Section 3.1) and the elastic modulus is computed. Usually material constants are used to determine static deflections, but in this case the procedure is reversed. The finite element procedures in Section 3 are identical to this except that the deflection comes from a finite element analysis rather than experimental data.

Dynamic effective material constants, or constants derived from a dynamic analysis, are calculated in much the same way as the static effective material constants. The difference is in the governing equation. Modal frequencies from a finite element analysis are entered into the equation from Section 4.1 and the effective stiffness is extracted.

4.2 Finite Element Results

The finite element analysis showed that plate modal frequencies are a function of ligament efficiency (Fig. 14). In addition, results show that dynamic effective material

constants are very different from static effective material constants (Fig. 15). Two sets of static effective material constants are included in Fig. 15 to highlight this fact. One set of data was generated from an ANSYS model of a perforated plate while the other set was generated using the combination of a solid plate and static effective material constants. Table 3 summarizes the differences in static versus dynamic stiffness.

Table 3. Comparison of static stiffness to dynamic stiffness for a simply supported plate with a square penetration pattern ($\nu = 0.30$).

Analysis Type	Ligament Efficiency (μ)	Effective Stiffness / Stiffness D^*/D	Percent Difference (static vs. dynamic)
Static	0.8	0.963	
Dynamic Mode 1	0.8	0.939	2.5%
Static	0.6	0.874	
Dynamic Mode 1	0.6	0.760	13.0%
Static	0.4	0.769	
Dynamic Mode 1	0.4	0.542	29.5%
Static	0.2	0.662	
Dynamic Mode 1	0.2	0.318	108.2%

5. Conclusions

Experimental and theoretical effective stiffness values for tubesheets agree well with stiffness values determined from FE deflection analysis of statically loaded perforated plates. A comparison of theoretical and experimental values with FE results for stiffness showed a fractional percentage difference at a ligament efficiency of 0.20, increasing to a 4.3 % difference at a ligament efficiency of 1.60. However, modal frequencies based upon equivalent static stiffness values do not compare well with modal frequencies from FE analysis. The results have identified a new category of dynamic effective stiffness that should generally be used in vibration problems in lieu of traditional static values.

Acknowledgment

Computer support for this research has been provided in part by the National Science Foundation.

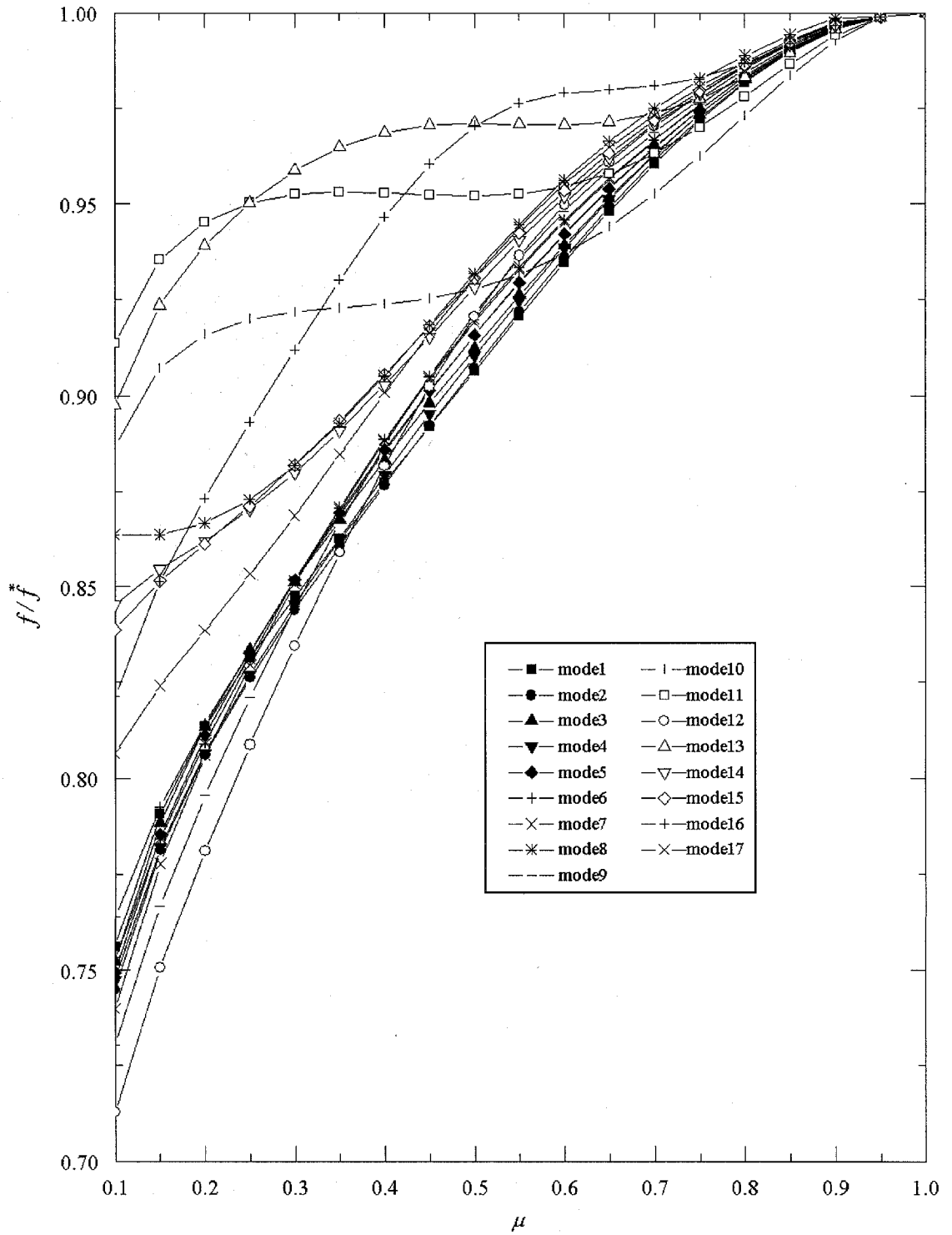


Fig. 14. Dimensionless frequency versus ligament efficiency for a square simply supported plate with a square perforation pattern.

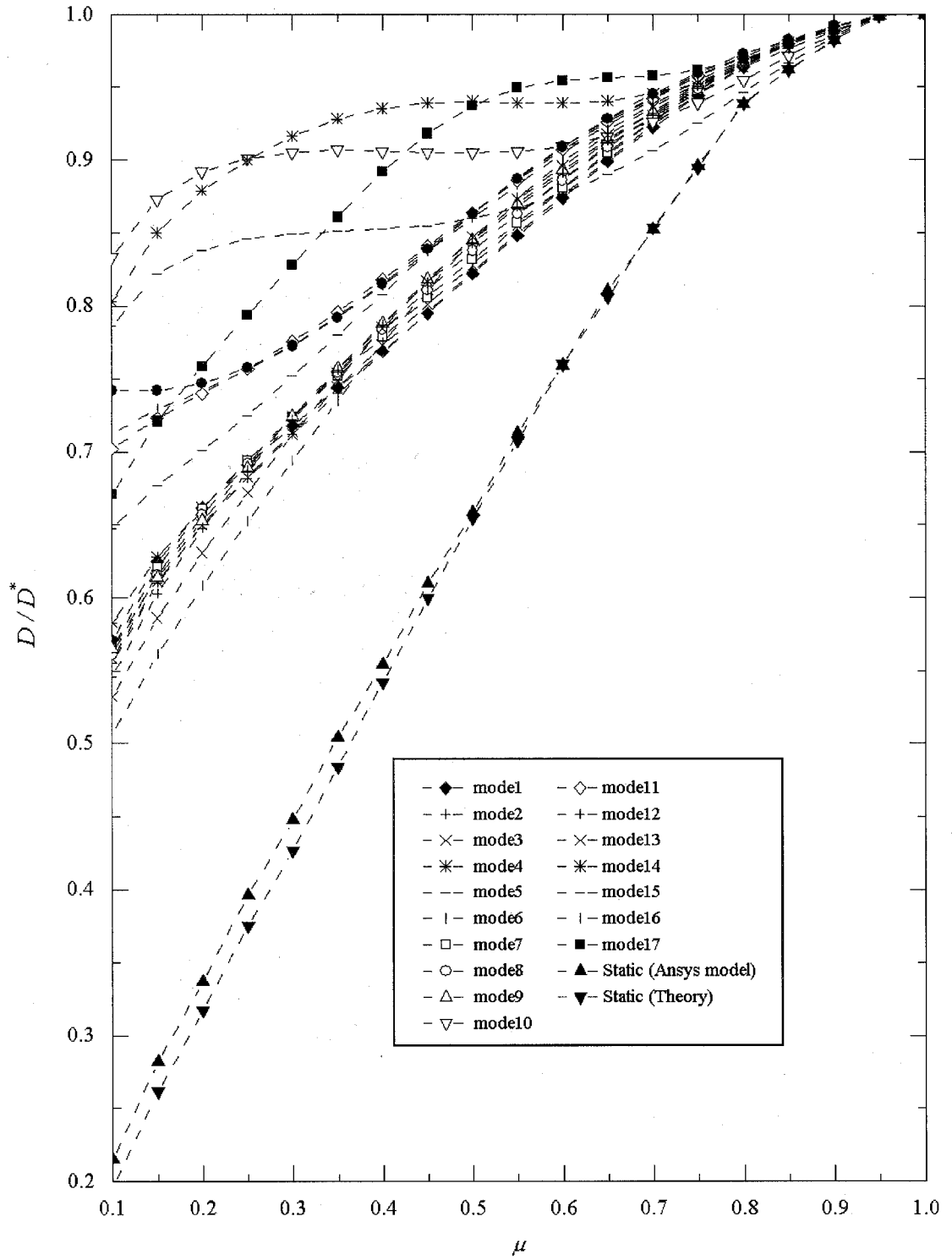


Fig. 15. Dimensionless effective dynamic stiffness versus ligament efficiency for a square simply supported plate with a square perforation pattern.

6. References

- [1] Osweiller, F., "Evolution and Synthesis of the Effective Elastic Constants Concept for the Design of Tubesheets," *Journal of Pressure Vessel Technology*, Vol. 111, pp. 209-217, 1989.
- [2] Nelms, H. A., "Flow-Induced Vibrations: A Problem in the Design of Heat Exchangers for Nuclear Service," in *Flow-Induced Vibration in Heat Exchangers*, Winter Annual Meeting of ASME, New York, NY, p. 10, 1970.
- [3] O'Donnell, W. J., "A Study of Perforated Plates with Square Penetration Patterns," *Welding Research Council Bulletin No. 124*, pp. 1-13, 1967.
- [4] Powers, J. P., "Structural and Fatigue Analysis of the Sandia Laboratory Microfusion Reaction Chamber," M.S. thesis, University of Wisconsin—Madison, Madison, WI, 1991.
- [5] Engelstad, R. L., Cousseau, P. L., Kulcinski, G. L., "Near Term ICF Target Chambers," *Fusion Power Associates FPA-96-2*, 1996.
- [6] Slot, T., "Stress Analysis of Thick Perforated Plates," Technomic Publishing, Westport, Conn., 1972.
- [7] ANSYS Engineering Analysis Systems User's Manual, Rev. 5.3, 1996.
- [8] Duncan, "The Structural Efficiency of Tube-Plates for Heat Exchangers," *Proceedings of the IME*, Vol. 169, 1955.
- [9] Ugural, A. C., "Stresses in Plates and Shells," McGraw-Hill, Inc., pp. 75-77, 1981.
- [10] Leissa, A. W., "Vibrations of Shells," NASA SP-288, 1973.
- [11] Meguid, S. A., Kalamkarov, A. L., Yao, J., Zougas, A., "Analytical, Numerical, and Experimental Studies of Effective Elastic Properties of Periodically Perforated Materials," *Journal of Engineering Materials and Technology*, Vol. 118, pp. 43-48, 1996.
- [12] Cook, R. D., Malkus, D. S., Plesha, M. E., "Concepts and Applications of Finite Element Analysis," Third Edition, John Wiley & Sons, Inc., 1989.
- [13] Sampson, R. C., "Photoelastic Frozen Stress Study of the Effective Elastic Constants of Perforated Materials," WARD-DLE-319, Office of Technical Service, Dept. of Commerce, Washington, D.C., 1959.